

GEOMETRIC AND RADIOMETRIC MODELING OF THE MARTIAN SURFACE BASED ON OBJECT SPACE MATCHING AND PHOTOCLINOMETRY

S. Gehrke^{a,b}

^a TU Berlin, Geodesy and Geoinformation Science, Straße des 17. Juni 135, D-10623 Berlin, Germany

^b North West Geomatics, Pixelgrammetry Group, 212-5438 11th Street NE, Calgary, AB T2E 7E9, Canada
stephan.gehrke@pixelgrammetry.com

Commission IV, WG IV/7

KEY WORDS: Planetary Cartography, Radiometry, Matching, Visualization, DEM/DTM, Orthoimage, Atmosphere

ABSTRACT:

The unique image data of the *High Resolution Stereo Camera* (HRSC) on *Mars Express* enable for systematic derivation of Digital Terrain Models (DTMs) and orthoimages. Consequently, several photogrammetric processing algorithms have been investigated with HRSC imagery. The results form the basis for further research including photometric analysis. Within this paper, an integrated approach for photogrammetric and photometric modeling is presented: the combination of matching in object space and photoclinometry. Using both geometric and radiometric image properties, geometry (DTM) and radiometry (Hapke reflectance parameters) of the Martian surface as well as atmospheric properties are jointly derived. Results will be shown for the Gusev crater southern hills and for an area with two small impact craters.

KURZFASSUNG:

Die einzigartigen Bilddaten der *High Resolution Stereo Camera* (HRSC) auf *Mars Express* ermöglichen die systematische Ableitung Digitaler Geländemodelle (DGMs) und Orthobilder. Folglich sind verschiedene photogrammetrische Verfahren zur HRSC-Datenprozessierung untersucht worden. Die Ergebnisse bilden die Basis für weitere Forschungen wie die photometrische Analyse. In diesem Paper wird ein integrierter Ansatz zur photogrammetrischen und photometrischen Modellierung präsentiert: die Kombination von Matching im Objektraum und Photoklinometrie. Unter Ausnutzung der geometrischen und radiometrischen Bildeigenschaften werden Geometrie (DGM) und Radiometrie (Hapke-Reflexionsparameter) der Mars-Oberfläche sowie Atmosphäreigenschaften gemeinsam abgeleitet. Ergebnisse werden für das Gusev-Bergland und für ein Gebiet mit zwei kleinen Einschlagkratern gezeigt.

1. INTRODUCTION

The *High Resolution Stereo Camera* (HRSC) on board of the European *Mars Express* mission is imaging Mars since January 2004. After four years, HRSC is still unique regarding its ability to provide multiple stereo and full color within each imaging sequence. Altogether, this line scanner features nine bands in stereo angles between $\pm 18.9^\circ$ (Fig. 1), five of them panchromatic and four colors: red, green, blue, and infrared. The entire data set is converted into Digital Terrain Models (DTMs) and orthoimages, which form the basis for map products and various scientific researches (JAUMANN et al., 2007). Besides this systematic processing, several photogrammetric approaches have been investigated with HRSC imagery and recently compared in the *HRSC DTM Test* (ALBERTZ et al., 2005; HEIPKE et al., 2007); almost all of them involve either image matching or photoclinometry, which is also known as shape-from-shading. An entirely different approach for HRSC data processing is investigated by the author: *Facets Stereo Vision*, an algorithm for matching in object space (WROBEL, 1987; WEISENSEE 1992). It integrates traditionally consecutive steps of (image) matching, point determination, surface reconstruction, and orthoimage generation and implicitly allows for regarding the connections between geometric (DTM) and radiometric surface properties (basically, an orthoimage). First results for Mars have been published by GEHRKE & HAASE (2006) and GEHRKE (2007). In the context of this paper, significant enhancements of this approach – which are especially necessary but also very promi-

sing when applied on planetary surfaces like Mars – are suggested. Most important is the integration of object space matching, i.e., absolute height determination from image geometry, and photoclinometry, i.e., relative height (inclination) determination from image radiometry. Similar approaches have been presented in computer vision by FUA & LECLERC (1995) and in planetary science by LOHSE et al. (2006).

As photoclinometry has to be based on an appropriate reflectance model – in the context of this investigation: HAPKE (1993) –, the new approach allows not only for geometric surface modeling but for the integrated determination of material (reflectance) parameters. Moreover, atmospheric properties – optical depth and the influence of ambient light – can be derived together with surface models and, therefore, also corrected for.

In the following, geometric and radiometric models suited to describe the Martian surface as well as the integrated approach that allows for determining these models are described. Results are presented for a sub-area of Gusev crater, in which the *Mars Exploration Rover* (MER) *Spirit* operates, and for two small impact craters at the resolution limit of HRSC DTMs.

2. SURFACE MODELS AND IMAGE FORMATION

Any natural surface can be described by its shape and composition, i.e., in terms of a DTM and material parameters. These continuous properties are modeled in facets with appropriate interpolation functions, within this investigation by bilinear inter-

polation. Facets of an orthoimage – usually the model with the highest resolution – are named surfels (surface elements); their size should be related to the ground resolution of the original imagery. The radiometry of an orthoimage is influenced by surface geometry and material reflectance properties in combination with illumination and viewing conditions (Fig. 1).

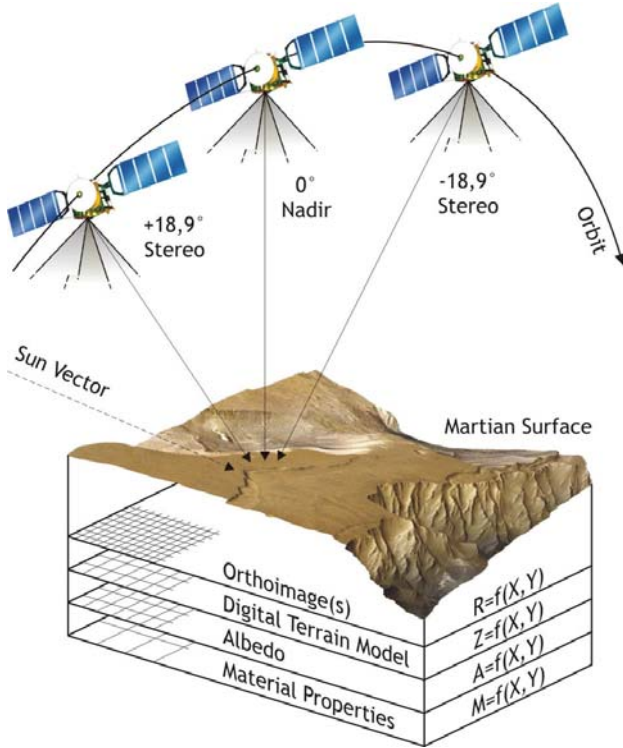


Fig. 1: HRSC imaging configuration and models for the Martian surface.

For remote sensing applications, which are based on observed reflectance, material properties are usually described as parameters of a bidirectional reflectance model. A physically meaningful description of planetary surfaces is achieved through the *Hapke Model* (HAPKE, 1993) that can be written as:

$$R = \frac{w}{4} \frac{\cos \theta_i}{\cos \theta_i + \cos \theta_r} \{P(\alpha) + H(\theta_i)H(\theta_r) - 1\} S(\bar{\theta}) \quad (1)$$

R is the radiance factor (RADF) as defined by HAPKE (1993). It depends on illumination and observation geometries – local incidence angle θ_i , viewing angle θ_r , and phase angle α – and material properties: particle single scattering albedo w (brightness) in combination with the angular distribution P , multiple inter-particle scattering modeled by the geometry-dependent H -Functions, and macroscopic roughness, i.e., the average surface tilt θ . Equation (2) does not take into account the opposition effect (a strong reflectance surge for $\alpha \rightarrow 0$), as the necessary observations are not available by HRSC unless a larger number of suitable orbits is used (cp. JEHL et al., 2008). That is, however, outside the scope of this investigation (see chapter 6). A widely used description of the angular distribution of particle scattering is the *Double Henyey-Greenstein* phase function:

$$P(\alpha) = c \frac{1-b^2}{(1-2b \cos \alpha + b^2)^2} + (1-c) \frac{1-b^2}{(1+2b \cos \alpha + b^2)^2} \quad (2)$$

The two terms in equation (3) are related to forward and backward scattering, both probability distributions in terms of ellipses whose shape is defined by b with $0 \leq b \leq 1$; $b = 0$ (circle) refers to evenly distributed scattering, $b \rightarrow 1$ to pronounced lobes. Forward and backward scattering are weighted by c with $0 \leq c \leq 1$. Although these parameters are empirical, they are suited to describe particle shape, surface, and interior, i.e., the density of internal scatterers (cp. Fig. 5).

For HRSC, radiance factors of all image pixels can be derived from the recorded intensities (JAUMANN et al., 2007); they are treated as observables: R_{HRSC} . These values result from surface reflectances R , influenced by atmospheric attenuation and ambient light. The first effect is multiplicative, depending on the atmospheric optical depth τ and the path length, i.e., the reflectance angle $\theta_{r(Level)}$ with respect to the surface normal (level surface). Ambient light causes an additive contribution ΔR_A . Then, the radiometric relation between surface reflectances and observed values may be modeled (e.g., HOEKZEMA et al., 2006):

$$R_{HRSC} = R \cdot \exp\left(-\frac{\tau}{\cos \theta_{r(Level)}}\right) + \Delta R_A \quad (3)$$

The geometric relation between an object point (X,Y,Z) and an image point (x,y) are the well-known collinearity equations:

$$\begin{aligned} x &= c \frac{r_{11}(X - X_0) + r_{21}(Y - Y_0) + r_{31}(Z - Z_0)}{r_{13}(X - X_0) + r_{23}(Y - Y_0) + r_{33}(Z - Z_0)} \\ y &= c \frac{r_{12}(X - X_0) + r_{22}(Y - Y_0) + r_{32}(Z - Z_0)}{r_{13}(X - X_0) + r_{23}(Y - Y_0) + r_{33}(Z - Z_0)} \end{aligned} \quad (4)$$

HRSC interior orientation consists of the focal length c ; position and attitude are given through (X,Y,Z) and the elements (r_{11}, \dots, r_{33}) of the rotation matrix, respectively. It has to be pointed out that each individual image line features its own exterior orientation. Both exterior and interior orientations are known from bundle adjustment (SPIEGEL & NEUKUM, 2007).

3. FACETS STEREO VISION

Facets Stereo Vision is a powerful approach for matching in object space. It has been developed since the late 1980s, mainly by WROBEL (1987) and WEISENSEE (1992). The application of the basic algorithm to HRSC on *Mars Express* images is discussed in detail by GEHRKE & HAASE (2006) and GEHRKE (2007).

3.1 The Approach for HRSC Data Processing

Geometric surface modeling from HRSC image data in this context is based on the indirect algorithm of *Facets Stereo Vision* according to WEISENSEE (1992), which has been adapted to *Mars Express* orbit and HRSC line scanner geometry.

The algorithm starts with the definition of appropriate orthoimage surfels and DTM facet sizes. Then, so-called pseudo orthoimages (pseudo observables) R are resampled for each HRSC band using equations (4); the necessary starting heights Z^0 are taken from the *Mars Orbiter Laser Altimeter* (MOLA) DTM (SMITH et al., 2001). After local contrast and brightness adaptation, an average orthoimage R^0 is derived as the average of all HRSC bands. Depending on DTM quality, the individual pseudo orthoimages will show lateral displacements (therefore the term “pseudo”). These are reduced by deriving corrections dZ for all DTM posts by least squares adjustment based on equa-

tion (5) – involving bilinear interpolation for surfels within a particular DTM facet. See GEHRKE & HAASE (2006) for formal derivation and further details.

$$R = R^0 + \left[\frac{\partial R^0}{\partial X} \frac{X - X_0}{Z^0 - Z_0} + \frac{\partial R^0}{\partial Y} \frac{Y - Y_0}{Z^0 - Z_0} \right] dZ \quad (5)$$

The entire *Facets Stereo Vision* algorithm has to be carried out iteratively, starting with the resampling using enhanced DTM heights, until no significant height changes remain. It has been proven effective to start up with a comparatively coarse model (MOLA DTM resolution) and increase it step by step (Fig. 2).

3.2 Regularization Aspects

The basic algorithm becomes weak in smooth regions that comprise only little texture or small contrast differences – areas that frequently occur on the dust-covered Martian surface. Thus, the adjustment has to be stabilized by additional assumptions. This may be realized by introducing terrain-dependent restrictions to surface curvature (WROBEL et al., 1992; GEHRKE 2007).

While such regularization significantly reduces noise and overcomes DTM outliers, in particular when locally weighted by surface properties, such conditions are only fictitious. This lack could be overcome by fully using all radiometric image information, i.e., the observed radiance factors of each pixel, and to combine matching in object space with photoclinometry.

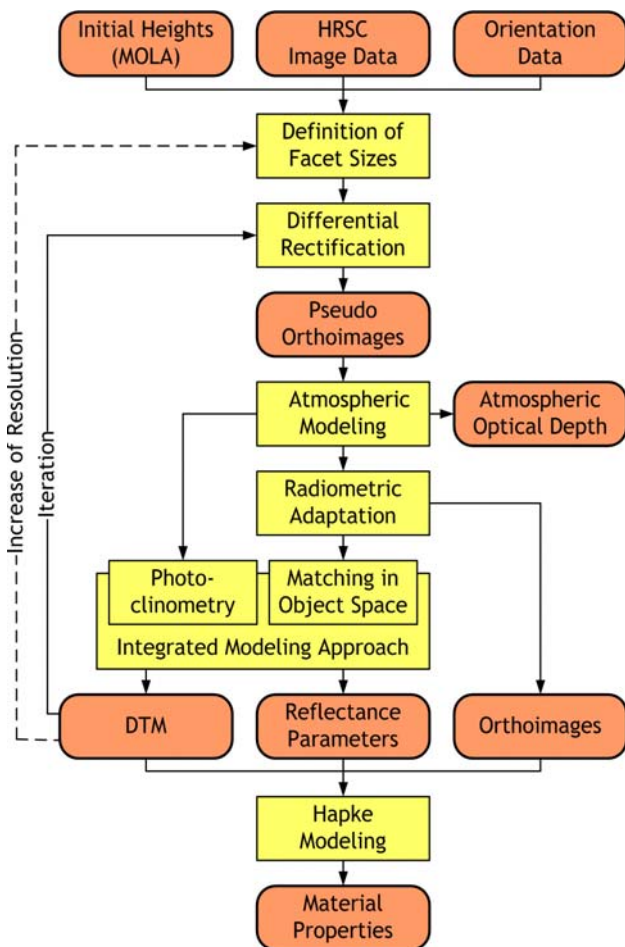


Fig. 2: Integrated approach for geometric and radiometric modeling of the Martian surface.

4. THE INTEGRATED APPROACH

4.1 Combination of Facets Stereo Vision and Photoclinometry

Radiometric image formation is described by a surface reflectance model combined with an atmospheric model (see 4.3 for the latter). Assuming, the reflectance model and its parameters are known, local surface normal vectors can be derived – see equation (1). Since this equation is in the form of (5), it readily allows for the integration of photoclinometry into *Facets Stereo Vision* (5), once local surfel inclinations in (1) are expressed in terms of dZ , again, with bilinear interpolation within the DTM. Such an approach nicely combines the advantages of both matching, which provides reliable absolute heights for well textured image parts (global accuracy), and photoclinometry, which leads to relative heights (local accuracy) and is suited to bridge matching gaps. This goal is achieved by weighting the two algorithms in the combined least squares adjustment depending on local image texture, practically carried out using radiance factor gradients in X and Y that are already part of (5).

4.2 Radiometric Surface Modeling

In most cases, the assumption of known reflectance parameters does not hold true; they have to be determined. Here lies the major advantage of the combined approach: If matching leads to (some) reliable heights that constrain inclination, reflectance parameters may be derived within the photoclinometry part of the adjustment. This ability requires certain relief energy as well as good image texture.

However, the *Hapke* parameters, described in chapter 2, tend to be highly correlated and the derivation along with DTM and orthoimage will very likely fail. Therefore, the empirical two-parameter *Lunar-Lambert-Model* – a suitable approximation for *Hapke*, proven throughout various theoretical and practical investigations (MCEWEN, 1991; KIRK et al., 2004) – is chosen as the radiometric surface description in this context:

$$R = A \left[2L \frac{\cos \theta_i}{\cos \theta_i + \cos \theta_r} + (1 - L) \cos \theta_i \right] \quad (6)$$

The normal albedo A in (6) is linked to the particle single scattering albedo w , the limb darkening parameter L to the surface roughness in the *Hapke Model* (1). Thus, based on the empirical reflectance resulting from the adjustment, physically meaningful *Hapke* parameters can be retrieved afterwards (Fig. 2).

4.3 Atmospheric Modeling

For an appropriate surface modeling, attenuation of the atmosphere (optical depth) and the influence of ambient light are to be regarded – cp. equation (5). While the latter can be integrated into the adjustment as an additional parameter, the optical depth is derived in advance since the related multiplicative term in (5) would highly correlate with the albedo factor in (6).

Optical depth can be derived by the *Stereo Method* (HOEKZEMA et al., 2006), which uses HRSC stereo bands: different angles result in different atmospheric path lengths and, according to equation (3), different influences of optical depth, which causes different image contrasts. Then – assuming identical ambient light and allowing only linear differences in surface reflectance between stereo angles – the optical depth could be derived from contrast differences, ideally from nadir and the outermost stereo band(s) as those feature the biggest path length difference.

4.4 Modeling Algorithm

The integrated approach, as shown in Fig. 2, enhances *Facets Stereo Vision* (chapter 3.1) with photoclinometry (4.1) and integrates the derivation of surface reflectance (2 and 4.2) and atmospheric properties (4.3). Depending on the actual investigation area, desired quality, and resolution, it might become useful or even necessary to constrain or omit individual parameters. In general, surface reflectance and atmospheric models are interchangeable and can be replaced. E.g., *Lambert's Model* may be used for very simple surface parameterization.

In practice, the complexity of the algorithm should be increased along with the increase of resolution. Photoclinometry is not necessary to obtain a coarse DTM, and meaningful photometric parameters can only be obtained if geometric details of the surface are modeled. In this context, it may still be useful to regularize the least squares adjustment as described in 3.2.

The integrated algorithm can be regarded as a complete surface modeling approach for Mars that makes use of all radiometric and geometric information contained in HRSC data. Because it is based on the entire image content – literally every pixel that is obtained in the investigation area –, it can be applied to small regions only, typically below 100x100 DTM facets.

5. APPLICATION

The integrated surface modeling algorithm has been implemented in MATLAB. It has been applied to several regions of Mars using HRSC imagery of different resolution obtained under various illumination and viewing geometries. In the following, two representative examples are discussed: a 25x25 km area of hills and mesas, which is located in southern Gusev, as well as a 2.8x2.8 km area containing two small impact craters.

5.1 Investigation Areas and HRSC Data

The described surface modeling approach can make use of panchromatic HRSC bands: stereo (S1/S2), photometry (P1/P2), and nadir (ND). (See chapter 6 for remarks on color.)

The Gusev area has been imaged multiple times (cp. JEHL et al., 2008), e.g., during orbit 648 from very high altitudes (Fig. 3; Table 1). Although this inevitably leads to rather low ground resolutions, the major advantage is large stereo angles due to orbit curvature – up to 31.2° in comparison to nominal HRSC angles of 18.9°. Local viewing angles range from 0° to 60°. The illumination is generally low; it varies locally between 51° and 90°, casting some shadows. Such geometry potentially allows for the derivation of reliable atmospheric optical depth and surface reflectance. Therefore, radiometric results are discussed in-depth.

Table 1: Overview of HRSC bands and viewing geometries

Area:	Gusev Southern Hills		Two Craters	
Orbit:	648		894	
Band	Ground Resolution	Viewing Angle	Ground Resolution	Viewing Angle
S1	281 m/pixel	31.2°	36 m/pixel	21.6°
P1	289 m/pixel	21.4°	-	-
ND	165 m/pixel	2.1°	16 m/pixel	0.4°
P2	448 m/pixel	29.5°	-	-
S2	n/a	n/a	32 m/pixel	21.7°

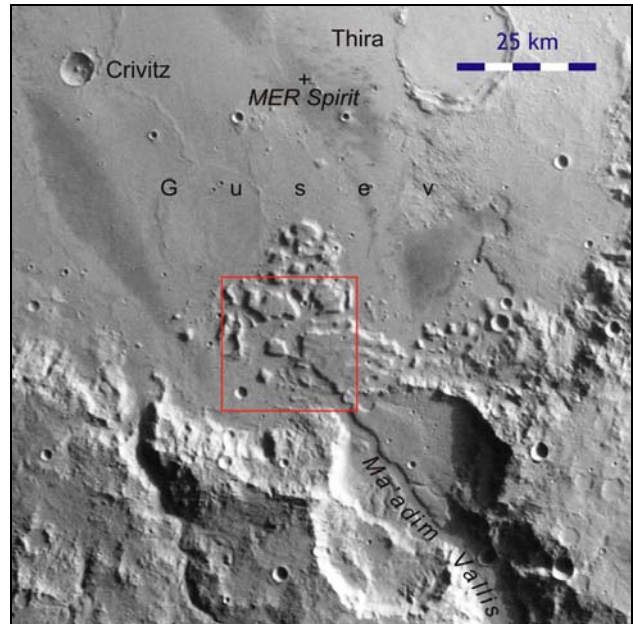


Fig. 3: Investigation area (red rectangle) within Gusev crater.

The second investigation area – two small craters in the Nanedi Valles region, imaged during orbit 894 (Fig. 6) – has been chosen to demonstrate the approach's strength in modeling fine surface details. With special emphasis on high resolution geometry, HRSC photometry bands with ground resolutions around 65 m/pixel (due to pixel binning) have not been used (Table 1).

5.2 Gusev Southern Highlands

For the Gusev area, surface radiometry and geometry as well as atmospheric properties have been successfully derived. The resulting DTM features a post spacing of 500 m (Fig. 4).

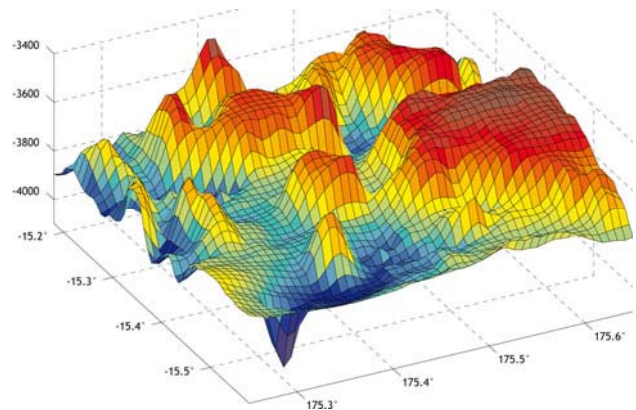


Fig. 4: Gusev hills DTM as color-coded perspective view.

The optical depth has been determined with $\tau = 1.55 \pm 0.06$, meaning that only 21% of the reflected light directly reached the nadir-looking detector. This number appears low but, however, it is well within the range that HOEKZEMA et al. (2006) derived for regions in and around Gusev crater.

Based on the integrated adjustment results, one *Hapke Model* has been calculated for the entire investigation area, excluding shadows. The initial approach involved all four parameters of equation (1); it lead to a large *c* value that was also highly correlated with the other phase function parameter, *b* (Table 2).

Table 2: Comparison of Hapke parameters obtained in the integrated approach with results of JEHL et al. (2006, 2008).

Par.	4 Parameter Model	3 Parameter Model	JEHL et al. (2006, 2008)
w	0,851 ± 0,002	0,869 ± 0,002	0,78 ... 0,88
b	0,141 ± 0,005	0,294 ± 0,002	0,20 ... 0,45
c	1,821 ± 0,042	1	0,45 ... 0,65
$\bar{\theta}$	29,5° ± 0,4°	32,3° ± 0,9°	25° ... 30°

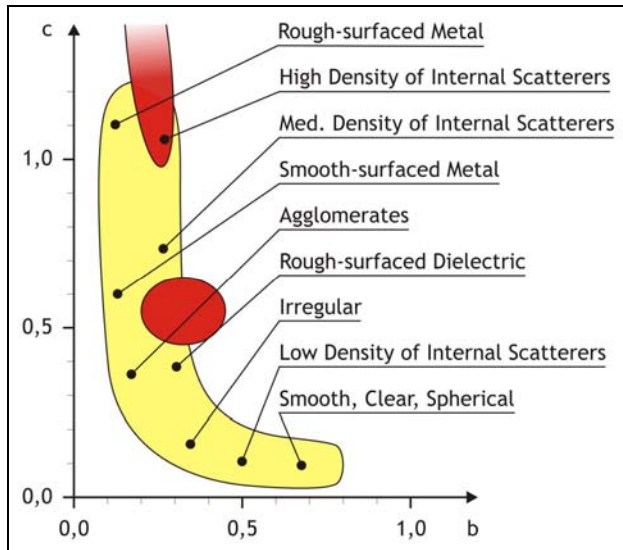


Fig. 5: Phase function plot: c against b (HAPKE, 1993). Typical values form an L-shaped area, which is shown in yellow with corresponding material properties. Gusev hills parameters as obtained here as well as those of JEHL et al. (2006, 2008) are marked in red – cp. Table 2.

A second, three parameter model has been calculated by constraining $c = 1$, which is the theoretical maximum (pronounced backscattering) while in practice values $c > 1$ occur along with low b values. The resulting b - c -plot and its relation to surface particle properties are illustrated in Fig. 5.

JEHL et al. (2006, 2008) have derived Hapke Model parameters from multiple HRSC orbits in the Gusev area. Although those studies did not account for the atmospheric optical depth, they are used for comparison – see Table 2 and Fig. 5. As a result, all parameters besides the already discussed c match very nicely. However, standard deviations seem to optimistic.

Radiometric analysis of the Gusev hills indicates that they are covered by bright particles (high albedo), which show pronounced backscattering due to a medium to high number of internal scatterers (cp. Fig. 5). The surface is comparatively rough.

5.3 Small Craters

Mars is characterized by a huge number of impact craters like those shown in Fig. 6 with sizes of approximately 700 m. This area has also been part of the HRSC DTM Test, based on the very same data set (orbit 894). One of the test results was that only 5% of craters below 1 km in diameter have been resolved, even in the DTM considered as “best overall result in terms of accuracy and fine detail” (HEIPKE et al., 2007).

Based on the integration of matching and photogrammetry, a DTM with a post spacing of 50 m has been collected. Both craters have been successfully modeled, which is nicely illustrated in Fig. 6 by contour lines laid on top of the derived orthoimage as well as by two shaded relief views. The first one is calculated with the original illumination conditions; it appears almost like the orthoimage, because it basically “inverts” the photogrammetry part of the modeling algorithm. Most critical is not the direction of the illumination – and, depending on the reflectance model, viewing directions to a certain point – but the direction perpendicular to it: from equation (6), which is used for photogrammetry, follows that those facet tilts are less constrained (as they do not affect illumination angles). Thus, the respective shaded relief reveals a few local inaccuracies related to the illumination direction. Nevertheless, geometric characteristics of this area, in particular crater shapes, are clearly recognizable.

Absolute DTM accuracy can be checked by comparison with MOLA points, i.e., altimeter measurements with standard deviations of about 1 m in height for smooth terrain (SMITH et al., 2001). Heights at those point locations have been interpolated in the HRSC DTM. As a results, the mean height difference of the investigation area with respect to MOLA is -6.2 m. Deviations in individual points are independent from terrain – see, e.g., the crater area in Figure 6; the maximum of -21.0 m occurs near the border of the investigation area, where the DTM derivation is least constraint. The standard deviation of individual height differences is 7.1 m, which is well below the pixel size of 25 m for the orthoimage. (This value has been chosen in-between HRSC ground resolutions, cp. Table 1).

6. DISCUSSION, CONCLUSION, AND OUTLOOK

In conclusion, the combination of object space matching and photogrammetry, integrating geometric and radiometric modeling of the surface along with atmospheric parameters, indicates

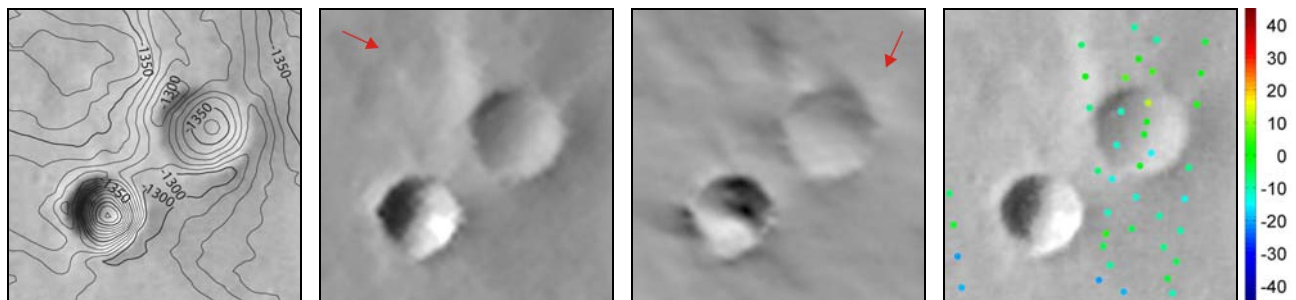


Fig. 6, from left to right: Overlay of orthoimage and contour lines; shaded relief with original illumination conditions (sun vector marked by the red arrow); shaded relief illuminated perpendicular to the original sun vector; color-coded height differences between HRSC DTM, derived with the integrated approach, and MOLA height measurements at MOLA spots.

to be a powerful approach, in particular with regard to quality: high DTM resolution with very good absolute accuracy, modeling of fine surface structures, and simultaneous derivation of material properties. *Hapke Model* parameters that have been derived based on the integrated approach nicely match with findings of independent photometric studies. The benefit from combining matching with photoclinometry is clearly visible in the resulting DTMs, especially in comparison to *HRSC DTM Test* data, which had been derived using either method. In particular, advantages over image matching are:

- A gridded DTM is the direct modeling result whereas it has to be interpolated from independent, irregularly distributed points after image matching.
- Therefore, local dependencies are implicitly regarded.
- The combination with photoclinometry introduces further local accuracy and bridges weak areas. It can be thought of as “terrain-dependent regularization”.

Major advantages compared to sole photoclinometry are:

- With terrain-dependent weighting against matching, photoclinometry can be targeted where necessary.
- DTM artifacts related to the illumination direction are reduced.
- Radiometric parameters for surface and atmosphere can be derived within the modeling approach.

However, the integrated approach is time-consuming and highly sophisticated; it can hardly be automated and is far from being operational, e.g., for processing entire HRSC orbits. Nevertheless, for small regions – that might be mosaicked, if desired – fine structures of the Martian surface can be modeled in high resolutions of up to 2x2 orthoimage surfels per DTM facet.

In both examples presented in this paper, the assumption of invariant radiometric surface properties has been made. In general, this has to be carefully evaluated, as unregarded radiometric variations will affect geometry! If applicable, parameters have to be modeled in facets as shown in Fig. 1.

In this context, it suggests itself to extend the approach to multiple HRSC orbits. Theoretically, this would substantially widen the range of illumination and viewing geometries and enable better radiometric surface modeling, e.g., in terms of deriving more than four parameters of the *Hapke Model* (see chapter 2). Moreover, wavelength-dependencies could be modeled based on redundant color information. However, different orbits are obtained at different times under different atmospheric conditions that would have to be modeled (and optical depth depends on wavelength!). Also the Martian surface might change, even over short periods of time caused by eolian activity.

REFERENCES

ALBERTZ, J., et al., 2005. HRSC on Mars Express – Photogrammetric and Cartographic Research. *Photogrammetric Engineering & Remote Sensing*, 71(10), pp. 1153-1166.

FUA, P., LECLERC, Y.G., 1995: Object-Centered Surface Reconstruction: Combining Multi-Image Stereo and Shading. *International Journal of Computer Vision*, 16(1), pp. 35-55.

GEHRKE, S., 2007. Zur geometrischen und radiometrischen Modellierung der Mars-Oberfläche aus HRSC-Daten. *Publikationen der DGPF*, 16, pp. 683-694.

GEHRKE, S., HAASE, I., 2006. An Integrated Approach for Orthoimage and DTM Generation Using Mars Express HRSC Data. *IAPRS*, 36(B4), pp. 326-332.

HAPKE, B.W., 1993: *Theory of Reflectance and Emittance Spectroscopy*. Cambridge University Press.

HEIPKE, C., et al., 2007: Evaluating Planetary Digital Terrain Models – The HRSC DTM Test. *Planetary and Space Science*, 55(14), pp. 2173-2193.

HOEKZEMA, N.M., et al., 2006: Atmospheric Optical Depths from HRSC Stereo Images of Mars. *Not yet published*.

JAUMANN, R., et al., 2007: The High Resolution Stereo Camera (HRSC) Experiment on Mars Express: Instrument Aspects from Interplanetary Cruise through Nominal Mission. *Planetary and Space Science*, 55(7-8), pp. 928-952.

JEHL, A., et al., 2006: Improved Surface Photometric Mapping across Gusev and Apollinaris from an HRSC/Mars Express Integrated Multi-Orbit Dataset: Implication on Hapke Parameters Determination. *37th LPS*, abstract #1219.

JEHL, A., et al., 2008: Gusev Photometric variability as seen from the Orbit by HRSC/Mars Express. *Not yet published*.

KIRK, R.L., et al., 2004: Comparison of USGS and DLR Topographic Models of Comet Borrelly and Photometric Applications. *ICARUS*, 167: 54-69.

LOHSE, V., et al., 2006: Derivation of Planetary Topography Using Multi-Image Shape-from-Shading. *Planetary and Space Science*, 54(7), pp. 661-674.

MC EWEN, A.S., 1991: Photometric Functions for Photoclinometry and Other Applications. *ICARUS*, 92, pp. 298-311.

SMITH, D.E., et al., 2001: Mars Orbiter Laser Altimeter: Experiment Summary after the first Year of Global Mapping of Mars. *Journal of Geophysical Research*, 106(E10), pp. 23689-23722.

SPIEGEL, M., NEUKUM, G., 2007: Simultaneous Adjustment of Interior and Exterior Orientation of HRSC on Mars Express. *Proceedings ISPRS WG IV/7 Workshop*, Houston.

WEISENSEE, M., 1992: Modelle und Algorithmen für das Facetten-Stereosehen. *DGK-Reihe C*, 374.

WROBEL, B.P., 1987. Facets Stereo Vision (FAST Vision) – A New Approach to Computer Stereo Vision and Digital Photogrammetry. *Intercommission Conference on Fast Processing of Photogrammetric Data*, Interlaken, pp. 231-258.

WROBEL, B.P., et al., 1992: Adaptive Surface Regularization – A New Method for Stabilization of Surface Reconstruction from Images. *IAPRS*, 29(B3), pp. 824-831.